HHS Public Access

Author manuscript

Brain Res. Author manuscript; available in PMC 2021 January 15.

Published in final edited form as:

Brain Res. 2020 January 15; 1727: 146571. doi:10.1016/j.brainres.2019.146571.

NMDA receptors containing GluN2C and GluN2D subunits have opposing roles in modulating neuronal oscillations; potential mechanism for bidirectional feedback.

Zhihao Mao[1], **Shengxi He**[1], **Christopher Mesnard**[1], **Paul Synowicki**[1], **Yuning Zhang**[1], **Lucy Chung**[1], **Alex I. Wiesman**[2], **Tony W. Wilson**[2], **Daniel T. Monaghan**[1,*]

[1]Department of Pharmacology and Experimental Neuroscience, University of Nebraska Medical Center, Omaha, Nebraska 68198-5800, USA

[2]Department of Neurological Sciences, University of Nebraska Medical Center, Omaha, Nebraska 68198, USA

Abstract

NMDA receptor (NMDAR) antagonists such as ketamine, can reproduce many of the symptoms of schizophrenia. A reliable indicator of NMDAR channel blocker action *in vivo* is the augmentation of neuronal oscillation power. Since the coordinated and rhythmic activation of neuronal assemblies (oscillations) is necessary for perception, cognition and working memory, their disruption (inappropriate augmentation or inhibition of oscillatory power or inter-regional coherence) both in psychiatric conditions and with NMDAR antagonists may reflect the underlying defects causing schizophrenia symptoms. NMDAR antagonists and knockout (KO) mice were used to evaluate the role of GluN2C and GluN2D NMDAR subunits in generating NMDAR antagonist-induced oscillations. We find that basal oscillatory power was elevated in GluN2C-KO mice, especially in the low gamma frequencies while there was no statistically significant difference in basal oscillations between WT and GluN2D-KO mice. Compared to wildtype (WT) mice, NMDAR channel blockers caused a greater increase in oscillatory power in GluN2C-KO mice and were relatively ineffective in inducing oscillations in GluN2D-KO mice. In contrast, preferential blockade of GluN2A- and GluN2B-containing receptors induced oscillations that did not appear to be changed in either KO animal. We propose a model wherein NMDARs containing GluN2C in astrocytes and GluN2D in interneurons serve to detect local cortical

Correspondence to: Daniel T. Monaghan.

*Author for correspondence.

Author Contributions

Zhihao Mao: Conceptualization, Investigation, Methodology, Data Curation, Formal analysis, Visualization, Writing-Original draft
Shengxi He: Investigation
Christopher Mesnard: Investigation
Paul Synowicki : Methodology, Investigation
Yuning Zhang: Investigation
Lucy Chung: Investigation
Alex I. Wiesman: Formal Analysis, Writing - Review & Editing
Tony W. Wilson: Formal Analysis, Writing - Review & Editing
Daniel T. Monaghan: Conceptualization, Methodology,Visualization, Writing - Review & Editing, Supervision, Funding acquisition

excitatory synaptic activity and provide excitatory and inhibitory feedback, respectively, to local populations of postsynaptic excitatory neurons and thereby bidirectionally modulate oscillatory power.

Keywords

electrocorticography; NMDA receptors; astrocyte; interneuron; schizophrenia; ketamine

1. Introduction

The rhythmic and coordinated activation of groups of neurons results in neuronal oscillations which are thought to be necessary for cognition, perception and working memory (Uhlhaas et al., 2008; Uhlhaas and Singer, 2012). Thus, it may be related to disease symptoms that in patients with schizophrenia, most studies (but not all) have found an increase in basal oscillatory power (Kikuchi et al., 2011; Spencer, 2011) and a decrease in task-related gamma oscillation power (Cho et al., 2006; Spencer et al., 2008). These electrophysiological changes are thought to underlie the reduced functional connectivity between brain regions observed in patients with schizophrenia using functional magnetic resonance imaging (fMRI) (Uhlhaas and Singer, 2015). Of note, there are also alterations in the task-related synchrony of oscillations between regions which may additionally contribute to symptoms (Block et al., 2007; Spencer et al., 2003; Spencer et al., 2009; Uhlhaas and Singer, 2015).

The ability of the NMDAR antagonists to mimic the spectrum of symptoms seen in schizophrenia (SZ) initiated the NMDAR hypofunction hypothesis of schizophrenia. This hypothesis is now supported by a variety of pharmacological and genetic studies in both humans and rodents, for reviews see (Kantrowitz and Javitt, 2010; Lisman et al., 2008). Consistent with this hypothesis, NMDAR channel blockers, or genetic deletion, has been associated with a robust augmentation of local neuronal oscillations and a deficit in interregional coherence (Dzirasa et al., 2009; Hakami et al., 2009; Korotkova et al., 2010; Pinault, 2008). Such augmentation of oscillations may be due to the preferential inhibition by NMDAR channel blockers of NMDARs on the fast-spiking parvalbumin-containing interneurons (Homayoun and Moghaddam, 2007). Their reduced excitation results in reduced GABAergic inhibition of pyramidal cells and thus increased excitatory activity. In short, NMDAR blockade may be disrupting cognition and perception by decreasing the signal to noise ratio of gamma oscillations, and / or altering oscillatory coherence between brain regions. Presently, it is not clear how different NMDAR subtypes participate in the oscillatory generators.

NMDAR complexes are composed of subunits from seven genes - GluN1, GluN2A-GluN2D, and GluN3A-GluN3B (Masu et al., 1993; Mishina et al., 1993; Monyer et al., 1994; Traynelis et al., 2010). These subunits assemble into hetero-tetrameric complexes in various combinations resulting in functionally distinct NMDARs. Many NMDARs are thought to be composed of two GluN1 subunits and two GluN2 subunits. The different alternatively-spliced GluN1 isoforms have largely similar pharmacological and

physiological properties whereas the GluN2 subunits confer distinct physiological, biochemical, and pharmacological properties to the NMDAR complex (Buller et al., 1994; Hollmann et al., 1993; Ikeda et al., 1992; Monyer et al., 1994; Sugihara et al., 1992; Vicini et al., 1998). For example, NMDAR containing GluN2C or GluN2D subunits display a reduced voltage-dependency due to a weaker Mg^{++} block, do not desensitize, have relatively high affinity for L-glutamate, and have slow-decaying current responses (Glasgow et al., 2015; Paoletti et al., 2013). These properties, combined with their varied developmental profiles and anatomical distributions (Alsaad et al., 2019; Watanabe et al., 1992; Watanabe et al., 1993a), imply that NMDARs containing these subunits may have a function in the CNS that is markedly distinct from the major GluN2A- and GluN2B-containing receptors.

In recent studies, we have found that the potent non-selective NMDAR antagonist MK-801 augmented gamma oscillations in GluN2C-KO mice more than in wildtype mice (Gupta et al., 2016). In contrast, in the GluN2D-KO mouse, ketamine-induced oscillations were greatly diminished (Sapkota et al., 2016). Since ketamine and MK-801 each have additional off-target activities (Briggs and McKenna, 1996; Clarke and Reuben, 1995; Sleigh et al., 2014), we sought in the present study to directly compare multiple NMDAR antagonists in both GluN2C-KO and GluN2D-KO mice to determine if the NMDAR antagonists effects on GluN2C-KO and GluN2D-KO mice are a general feature of NMDAR antagonists. Furthermore, since memantine has a potency, selectivity, and mechanism of action very similar to ketamine, but has less association with psychotomimetic effects, we were also interested to determine if memantine displays different effects on neuronal oscillations than other general NMDAR antagonists.

We find that NMDAR channel blockers, in general, have a larger effect on neuronal oscillations in the GluN2C-KO mouse than in wildtype (WT) mice and have very little effect in GluN2D-KO mice. In contrast to the results with channel blockers, preferential blockade of GluN2A- and GluN2B-containing receptors induced oscillations that did not appear to be changed in either KO animal.

2. Results

2.1 Baseline power in GluN2C-KO and GluN2D-KO mice

Electrocorticography (ECoG) recordings of awake WT, GluN2C-KO and GluN2D-KO mice displayed typical ECoG traces before and after drug administration. Relative to WT mice, GluN2C-KO mice, displayed higher average basal oscillatory power at all frequencies analyzed (30 – 200 Hz, $p < 0.001$, Fig. 1A; see section 4.5 for statistical analysis). A plot of the GluN2C/WT power ratio at different frequencies (Fig. 1B) suggests that basal power was especially elevated within the beta and low gamma range of 20 to 60 Hz. GluN2D-KO mice appeared to have higher basal power above 60 Hz, but there were no statistically significant clusters identified in the initial cluster analysis.

2.2 Ketamine

Ketamine administration is followed by increased cortical neuronal oscillations in mice (Fig. 2), as others have reported, for a review see (Hunt and Kasicki, 2013). The ketamine

response in WT and GluN2C/D KO mice has a rapid onset (~1–2 minutes) and begins to decay after 20 minutes (Fig. 2A), consistent with the known half-life for ketamine in mice (Sato et al., 2004). The rapid onset and rapid decay of the ketamine response suggests that these actions are mediated by ketamine and not an active metabolite of ketamine. The ketamine-induced increase in oscillatory power appeared to be greater in GluN2C-KO mice than in WT mice at low gamma frequencies. (Fig. 2B). Differences between WT and GluN2C-KO mice were most prominent between 30 and 60 Hz. From 30–60 Hz, WT mice displayed an 86 ± 20% (N=10) increase in power, whereas GluN2C-KO displayed an increase of 244 ± 36% (N=6). To identify frequency bands with statistically-significant differences between genotypes, potential frequency clusters were identified at the $p < 0.05$ level and then these were tested by permutation testing. WT and GluN2C-KO mice were found to be significantly different at the $p < 0.001$ level in the 31–45 and 51–63 Hz bands. In contrast, the ketamine response in GluN2D-KO mice was significantly reduced in the high gamma frequencies of 65–140 Hz as we have previously shown (Sapkota et al., 2016). Cluster analysis/permutation testing indicates that GluN2D-KO and WT mice were different at the $p < 0.001$ level for frequencies 56–74, 80–90, 111–117 and 129–131 Hz.

2.3 MK-801

Generally similar results were found for the ability of the potent NMDAR blocker MK-801 to induce oscillations in WT, GluN2C-KO, and GluN2D-KO mice. MK-801-induced augmentation of oscillations was greater in GluN2C-KO mice than in WT mice and greatly diminished in GluN2D-KO mice (Fig. 3). Statistical analysis indicates that WT and GluN2C-KO were different with a $p < 0.05$ for all frequencies between 45 Hz and 160 Hz (Figure 3C). Permutation testing of the identified clusters indicate that only 131–133 Hz ($p = 0.0013$) and 141–143 Hz bands ($p < 0.001$) were significant. In a manner generally similar to ketamine, MK-801-induced oscillations were weaker in GluN2D-KO mice than WT mice with $p < 0.05$ at most frequencies between 70 and 120 Hz. Permutation testing indicate that frequencies between 70–82, 90–94, and 97–105 Hz were significantly different at $p < 0.001$.

2.4 PCP

On average, PCP-induced oscillations were greater in the GluN2C-KO than in WT mice and largely diminished in GluN2D-KO mice (Fig. 4). However, there was more variability between individual animals and a relatively small number of available animals. Consequently, cluster analysis did not identify significant frequency clusters between WT and KO mice. Thus, the average PCP results are generally consistent with results from ketamine and MK-801 administration, but we cannot conclude that there was an effect of genotype.

2.5 Memantine

Memantine augmented neuronal oscillations in WT mice to a similar extent as did the other NMDAR channel blockers with an approximately 100% increase in power in the gamma frequency band (Fig. 5). The majority of this increase was eliminated in GluN2D-KO mice with the average GluN2D-KO response less than the WT response for all frequencies between 30 and 200 Hz. Cluster/permutation analysis indicted that there was less oscillatory power in the GluN2D-KO at $p < 0.001$ for frequencies 47–92, 162–168, 180–186, and 193–

197 Hz and at p = 0.0025 for 174–176 Hz. In contrast to GluN2D-KO mice, the average memantine-induced response in GluN2C-KO was larger than in WT mice. This augmentation above WT values was strongest between 65 and 90 Hz. Cluster/permutation analysis indicated significantly ($p < 0.001$) higher oscillatory power at 66–82 Hz and 86–92 Hz in the GluN2C-KO than in WT mice. In contrast to memantine, the average oscillatory response of the other NMDAR channel blockers was enhanced in the low gamma (30–60 Hz), though not always with statistical significance. High frequency oscillations (~140 – 160 Hz) were variably present after ketamine and MK-801 administration, but not observed after PCP or memantine.

2.6 NVP-AAM077 and Ro-25–6981

Studies have shown that blockade of NMDA receptors using the partially-selective GluN2A competitive antagonist NVP-AAM077 and selective blockade of GluN2B-containing receptors with the allosteric antagonist Ro-25–6981 can also enhance gamma oscillations although to a smaller extent than with channel blockers (Kocsis, 2012b). Consistent with these findings, both NVP-AAM077 and Ro-25–6981 were able to weakly enhance oscillatory activity. For both NVP-AAM077 and Ro-25–6981 there was no significant difference in response between WT and either GluN2C-KO or GluN2D-KO mice (Fig. 6). However, for NVP-AAM077, statistical analysis indicated that the possible drug-induced increase over baseline within each group of mice was not statistically significant. This appears to be due to the combination of a low response size and a low N. When all three animal groups were analyzed as a single group, NVP-AAM077 produced a statistically significant ($p < 0.001$) increase in oscillatory power over baseline in the 31.3 to 61.5 Hz band and a decrease in bands 98.6–141.6 and 143.6– 199 Hz ($p < 0.001$) as is suggested by Figure 6. The decrease in the higher frequency bands is distinct from the other compounds tested.

3. Discussion

3.1 NMDAR channel blockers induce stronger oscillations in GluN2C-KO mice and weaker oscillations in GluN2D-KO mice.

The synchronous, rhythmic activation of neuronal assemblies is necessary for perception, cognition, and working memory, and their disruption may reflect the underlying defects causing symptoms in schizophrenia and other neuropsychiatric disorders (Haenschel et al., 2009; Spencer et al., 2003; Uhlhaas et al., 2008; Uhlhaas and Singer, 2012). Blockade of NMDA receptor activity, or their genetic deletion, strongly modulates neuronal oscillations and impairs inter-regional coherence (Hakami et al., 2009; Hong et al., 2010; Kocsis, 2012b; Korotkova et al., 2010), thus providing a network mechanism for the NMDAR hypofunction hypothesis of schizophrenia. To date, however, the molecular/cellular mechanisms by which specific NMDAR subtypes contribute to neuronal oscillations are not well understood. In this study, we found that the deletion of GluN2C NMDAR subunits elevates basal oscillations and increases the ability of NMDAR channel blockers to augment neuronal oscillations. In the GluN2D-KO mouse, NMDAR channel blocking antagonists are less effective at inducing oscillations particularly in the high gamma frequencies. Thus, the differential effects of deleting GluN2C compared to GluN2D subunits appears to be a

general property of NMDAR channel blockers and are not likely to be due to individual off-target activities.

The GluN2A-preferring competitive antagonist NVP-AAM077 would block di-and triheteromeric receptors containing GluN2A (e.g. GluN1/GluN2A/GluN2B) since receptor activation requires two glutamate bound on each receptor(Benveniste and Mayer, 1991; Clements and Westbrook, 1991) and the GluN2B-selective allosteric antagonist Ro-25–6981 preferentially inhibit GluN2B di-heteromeric receptors and less potently inhibit GluN1/GluN2A/GluN2B receptors (Hansen et al., 2014; Hatton and Paoletti, 2005). Both of these antagonists were able to enhance neuronal oscillations, as has been reported by others (Kocsis, 2012b; Pittman-Polletta et al., 2018). The power of these induced-oscillations were not significantly different from WT in either the GluN2C-KO or GluN2D-KO. However, it is difficult to make a firm conclusion regarding the effect of genotype given the small effect size. The relatively small increase in oscillatory power evoked by NVP-AAM077 and Ro-25–6981 was of a magnitude similar to that reported by others (Kocsis, 2012b). This weak augmentation of oscillations by NVP-AAM077 is not likely to reflect an ineffective dose. The dosage used (20 mg/kg) is high compared to other *in vivo* studies in mice which found robust effects of NVP-AAM077 on memory and synaptic plasticity with 1.2 mg/kg (Busquets-Garcia et al., 2018) and 10 mg/kg (Hu et al., 2009; Yu et al., 2018) and on neuronal oscillations (10 and 20 mg/kg) (Kocsis, 2012a; Kocsis, 2012b; Pittman-Polletta et al., 2018). The dosage used is also high for comparable rat studies with significant pharmacological effects with 1.2 mg/kg (Dalton et al., 2012; Fox et al., 2006; Ge et al., 2010).

It is difficult to know the extent that different NMDARs would be blocked *in vivo* by NVP-AAM077. NVP-AAM077 is a weakly selective competitive antagonist with a potency order of GluN2A > GluN2C > GluN2D > GluN2B (with 2-fold to 12-fold selectivity in terms of K_i)(Feng et al., 2004). The apparent selectivity could be modestly improved *in vivo* since L-glutamate has 3- to 10-fold higher affinity at GluN2C and GluN2D-containing receptors than at GluN2A. Taken together, GluN2D-containing receptors would have the weakest sensitivity to NVP-AAM077 (high IC_{50}) if similar L-glutamate concentrations are seen at the different receptors (which is not known). Thus, the weak stimulation of oscillations, especially at higher frequencies, is consistent with NVP-AAM077 not inhibiting GluN2D-containing receptors and the possible lack of effect that knocking-out GluN2D has on NVP-AAM077-induced oscillatory activity. But further studies are necessary to define the role of GluN2A in neuronal oscillations.

These results are potentially consistent with the observation that channel blockers have a modest selectivity for GluN2C/D-containing receptors in the presence of Mg^{2+} (Kotermanski and Johnson, 2009). Thus, channel blocker-induced oscillations are altered by removal of GluN2C or GluN2D subunits whereas oscillations induced by blocking GluN2A- or GluN2B-containing receptors are not. These results are also consistent with the finding by Tricklebank and colleagues (Gilmour et al., 2009), that the behavioral effects of NVP-AAM077 and Ro 25–6981 differ from each other and from that of NMDAR channel blockers. However, since the augmentation of oscillations by NVP-AAM077 and Ro 25–

6981 was less than that produced by NMDAR channel blockers, it is more difficult to see a statistically-significant genotype effect when the effect size is small.

3.2 Possible mechanisms of GluN2D subunit modulation of gamma oscillations.

The ability of GluN2D-deletion to mostly eliminate NMDAR antagonist-induced gamma oscillations may be due to the loss of GluN2D subunits which in the cerebral cortex and hippocampus are expressed in GABAergic interneurons containing parvalbumin (PV) (Alsaad et al., 2019; Perszyk et al., 2016; Standaert et al., 1999; von Engelhardt et al., 2015; Yamasaki et al., 2014). PV cells participate in generating gamma oscillations (Buzsáki and Wang, 2012; Cardin et al., 2009) and the genetic deletion of NMDARs in these cells (Carlen et al., 2012; Korotkova et al., 2010) augments gamma oscillations. These findings are consistent with the observation that NMDAR channel blockers preferentially block interneurons (Homayoun and Moghaddam, 2007; Li et al., 2002) thus causing a disinhibition of downstream excitatory neurons.

GluN2D-containing NMDARs in thalamus (Alsaad et al., 2019; Watanabe et al., 1993b; Yamasaki et al., 2014) and the substantia nigra (Brothwell et al., 2008) could also be contributing to neuronal oscillations. NMDAR GluN2D subunits are expressed in the reticular nucleus of the thalamus and the midline thalamic nuclei (Alsaad et al., 2019; Buller et al., 1994; Watanabe et al., 1993b). Since these regions have extensive reciprocal connections with the cortex, thalamic GluN2D-containing NMDARs could have a role in modulating cortical gamma oscillations. GluN2D is also expressed in dopaminergic cells of the substantia nigra pars compacta (Brothwell et al., 2008). Interestingly, GluN2D-KO significantly reduces forebrain dopamine release in response to PCP and greatly reduces PCP-induced locomotor activity (Hagino et al., 2010). Likewise, GluN2D-KO significantly reduces ketamine-induced locomotor activity (Sapkota et al., 2016; Yamamoto et al., 2016) (but not MK-801 or PCP-induced locomotor activity on a different genetic background (Shelkar et al., 2019)). Stimulation of dopaminergic cells specifically increases high gamma oscillatory power (Lohani et al., 2019), an observation that is consistent with GluN2D-KO preferentially reducing ketamine-induced high gamma power (Sapkota et al., 2016). Thus, GluN2D-KO could be reducing NMDAR channel blocker-induced gamma oscillations by reducing dopamine release and, partially, by reducing locomotor activity (although, we sought to minimize locomotor-associated gamma as described in the methods).

3.3 GluN2C-containing NMDARs in astrocytes may be tonically enhancing neuronal oscillations.

The enhanced response to NMDAR antagonists in the GluN2C-KO may correspond to a loss of GluN2C subunits from astrocytes that provide positive feedback to neurons. Astrocytic processes near excitatory synapses can respond to L-glutamate spill-over during bursts of synaptic stimulation with an increase in intracellular calcium, for reviews see (Haydon, 2001; Verkhratsky et al., 1998). At least some of the astrocyte calcium response is thought to be due to NMDAR activation (Palygin et al., 2010). We have recently shown that in the telencephalon, GluN2C mRNA is commonly found in GFAP-positive glial cells and rarely found in neurons (Alsaad et al., 2019). This result is thus consistent with the original conclusions from *in situ* hybridization studies (Watanabe et al., 1993a) and with

transcriptome databases (Mancarci et al., 2017; Zhang et al., 2014). Pankratov and colleagues (Palygin et al., 2011) have shown that the GluN2C/D preferring NMDAR antagonist UBP141 (Costa et al., 2009) preferentially blocks NMDA-evoked currents in astrocytes. Since GluN2D mRNA is not found in glial cells in the cerebral cortex (Alsaad et al., 2019), these astrocyte currents are most likely to be mediated by GluN2C-containing NMDARs. This is consistent with the recent observation that agonist-evoked NMDAR currents in astrocytes are eliminated in the GluN2C-KO (Ravikrishnan et al., 2018). Thus, there are functional GluN2C-containing receptors in astrocytes that could be responding to bursts of synaptic excitation. In response to intracellular calcium elevations, astrocytes can exhibit calcium-dependent release of glial transmitters such as glutamate and ATP (Araque et al., 2000; Bezzi et al., 1998; Pasti et al., 2001). In turn, L-glutamate released from astrocytes has been shown to activate GluN1/GluN2B NMDARs synchronously in multiple postsynaptic neurons (Fellin et al., 2004), thus providing a mechanism by which astrocytes can provide a synchronizing feedback signal to excitatory neurons in response to strong synaptic stimulation (Angulo et al., 2004; Fellin et al., 2004). This hypothesis is consistent with our previous finding that burst stimulation, but not single stimulation, of the CA3-CA1 excitatory pathway results in a long-lasting postsynaptic NMDAR current that is blocked by both GluN2B and GluN2C/D antagonists (Costa et al., 2009; Lozovaya et al., 2004). According to this hypothesis, activation of GluN2C-containing NMDARs in astrocytes leads to depolarization of local pyramidal cells and enhances their excitatory activity and gamma oscillations.

It is noteworthy that recent studies have shown that astrocytes contribute specifically to the modulation of beta/low gamma in the 20 – 40 Hz range. Transgenic animals that cannot release L-glutamate from astrocytes display a depressed oscillatory power at 20–40 Hz (Lee et al., 2014). Conversely, in an *ex vivo* preparation, selective optogenetic stimulation of astrocytes depresses 20–40 Hz kainate-induced gamma oscillations in a manner blocked by A1 adenosine receptor antagonists (Tan et al., 2017). Astrocytes have also been proposed to modulate oscillations in this frequency range via synaptic glutamate-induced GABA release from astrocytes (Heja et al., 2012). Thus, astrocytes appear to be able to modulate 20–40 Hz oscillations in a bidirectional manner by releasing L-glutamate, ATP, and maybe GABA. If GluN2C-containing NMDARs regulate glial transmitter release, then their specific regulation of low gamma would be expected.

The greater oscillatory power in the GluN2C-KO in response to NMDAR blockers suggests that in the WT, GluN2C blockade normally suppresses oscillations (while blocking other NMDARs enhance oscillations). By this hypothesis, when a non-selective NMDAR antagonist is given to a WT mouse, there may be two opposing effects on gamma oscillations. NMDAR blockade of GluN2C-containing receptors reduces gamma oscillations (perhaps by reducing astrocyte glutamate-induced pyramidal cell depolarization). At the same time, NMDAR blockade of other NMDARs enhances neuronal oscillations (perhaps in part by blockade of GluN2D-containing NMDARs on fast-spiking GABAergic interneurons). Then when NMDAR blockers are given to the GluN2C-KO, the GluN2C blockade-mediated inhibition of gamma oscillations is absent, resulting in stronger oscillations due to the unopposed blockade of other NMDARs.

3.4 GluN2C- and GluN2D-containing NMDARs are ideal for producing tonic currents in response to low glutamate concentrations.

We propose that GluN2C- and GluN2D-containing NMDAR subtypes have distinct, critical roles in modulating neuronal oscillations due to their distinctive physiological and anatomical properties. Compared to GluN2A/B-containing NMDARs, GluN2C- and GluN2D-containing NMDARs have higher affinity for L-glutamate, show less voltage-dependency due to reduced Mg^{2+} sensitivity, have slow-decaying currents, and they do not desensitize (Glasgow et al., 2015; Krupp et al., 1998; Traynelis et al., 2010; Wyllie et al., 2013). Thus these receptors are well suited for being sensors of low concentrations of extracellular glutamate and they can retain their activity under tonic or fast-spiking activity and in turn provide a tonic NMDAR current response as seen in interneurons (Povysheva and Johnson, 2012; Riebe et al., 2016). With GluN2C in astrocytes, and GluN2D in GABAergic interneurons, these receptors can provide excitatory feedback, or inhibitory feedback, respectively, to the local ensemble of excitatory neurons in response to local excitatory drive. NMDARs containing GluN2C or GluN2D subunits represent numerically minor NMDAR subtypes in the forebrain. Thus, their potential ability to differentially modulate neuronal oscillations, while minimally impacting the major populations of NMDARs that are involved in a variety of other processes, suggests that these receptors could be useful targets for therapeutic applications.

4. Experimental Procedure

4.1 Surgery

All procedures were approved by the University of Nebraska Medical Center's Institutional Animal Care and Use Committee (IACUC) in compliance with the National Institutes of Health guidelines. 12–16 weeks old WT, GluN2C-KO and GluN2D-KO mice were surgically implanted with tripolar electrodes (MS333/2; Plastics One, Roanoke, VA) under xylazine/ketamine/ acepromazine anesthesia as required by IACUC regulations. Two holes were made in the skull 3 mm posterior to bregma at 1 mm and 2.5 mm lateral. Two electrodes were placed in the medial hole onto the dura surface near the retrosplenial cortex, and the third electrode was placed in the lateral hole for ground. The electrodes were secured to the skull as described elsewhere (Jeffrey et al., 2013).

4.2 Drugs

We used the general NMDAR antagonists: ketamine (30mg/kg, Par Pharmaceutical, Spring Valley, New York or Hospira, Inc., Lake Forrest, IL), MK-801 (0.2 mg/kg, kindly provided by Merck & Co.), memantine (20 mg/kg), and PCP (3mg/kg, Sigma-Aldrich, St. Louis, MO) and NMDAR subunit-selective antagonists: NVP-AAM077 (20 mg/kg, kindly provided by Novartis) and Ro25–6981 (30 mg/kg, Tocris). All drugs were dissolved in saline. The dosage of each drug was determined by prior experiments or literature values (Busquets-Garcia et al., 2018; Hu et al., 2009; Hunt et al., 2006; Kocsis, 2012b; Lesuis et al., 2019; Mikics et al., 2017; Phillips et al., 2012; Yu et al., 2018). Ketamine is typically used in the 5–50 mg/kg (i.p.) range in ECoG experiments with many studies using 20–25 mg/kg(Hunt and Kasicki, 2013). In our preliminary studies we found that the subanesthetic ketamine dose of 30 mg/kg gave a more robust augmentation of oscillations than 5 mg/kg, so further experiments used

the 30 mg/kg dosage. PCP is commonly used at 0.25 mg/kg to 10 mg/kg. We used 3 mg/kg because preliminary experiments found that this dosage gave more robust and reproducible oscillatory augmentation than with 1 mg/kg and responses that were of a similar magnitude to that of the other channel blockers. MK-801 is commonly used in the 0.05 to 0.25 mg/kg range, we found 0.2 mg/kg gave a reproducible, robust augmentation of oscillations. Memantine results in NMDAR-related behavioral effects in the 2.5 to 30 mg/kg range (Zhu et al., 2015; Havolli et al., 2017; Kakefuda et al., 2016). In our experiments, 20 mg/kg memantine gave clear augmentation of gamma oscillations comparable in magnitude with the other channel blockers. We selected concentrations near the high end of the ranges used in behavioral experiments. While there is evidence that some channel blockers have somewhat reduced augmentation of oscillation at the highest doses (Hiyoshi et al., 2014), for each of the channel blockers, the values we used are very similar to the optimal concentrations found for these agents in the enhancement of rat gamma oscillations (Hiyoshi et al., 2014). The dosage used for Ro-25–6981(30 mg/kg) in this study was high or comparable to other studies in mice in which robust pharmacological effects on NMDARs were observed, 3 and 10 mg/kg (Lesuis et al., 2019), 6 mg/kg (Busquets-Garcia et al., 2018; Zhang et al., 2013) and comparable to that used in augmenting neuronal oscillations(Kocsis, 2012a; Kocsis, 2012b; Pittman-Polletta et al., 2018). Dosage used and receptor subtype selectivity for NVP-AAM077 is discussed in the discussion.

4.3 ECoG Recordings

At least one-week after electrode implant surgery, animals in their home cage were placed inside a surrounding Faraday cage, the electrode assembly was connected to a commutator by a cable and the animals were allowed to acclimate for 10 minutes. ECoG recordings were made with a DP-311 differential amplifier using a sampling rate of 2000 Hz (Warner Instruments, Hamden, CT) with high-pass/low-pass filters set at 0.1 and 300 Hz and digitized/recorded (Digidata 1400, pClamp 10; Molecular Devices, Sunnyvale, CA). After 30 minutes of baseline recordings, the animals were injected i.p. with NMDA antagonists or saline and recorded for 60–90 minutes after the injection. Some recordings were paused during drug administration and then resumed within 2 minutes using the same recording conditions. Time-frequency spectrograms (e.g. Figs. 2–5) revealed that the ketamine response begins to decay after 20 minutes whereas the other agents had a sustained response for at least 90 minutes (results shown up to 60 minutes). Unlike the other agents which initiated a response in 2–5 minutes, MK-801's response was delayed by 10–15 minutes post-injection. For ketamine, the power spectrum was sampled between 5 and 30 minutes, for MK-801 between 15 and 90 minutes. Other antagonists were sampled between 5 and 90 minutes. Antagonists other than ketamine augment oscillations for several hours at these doses (Kocsis, 2012b). As previously described (Sapkota et al., 2016), to reduce movement-associated gamma oscillations, power measurements were obtained for awake animals at rest as noted in observer notes and by movement-induced recording artifacts caused by the tethered cable's movement. Our impression is that the tethered cable reduced animal movement, but this was not quantified.

4.4 Data Analysis

From the continuous recordings, several random 10-second segments were obtained during both the pre-drug baseline period and in the with-drug period and then analyzed. Power spectrum analysis was performed with Clampfit (Molecular Devices) using a Hamming window with 50% overlap. The power spectrum from the baseline and post-drug responses were averaged separately and then expressed as a post-drug/baseline ratio. These ratios were then averaged for each genotype/drug condition. Spectrogram analysis was performed by Neuroexplorer software (Nex Technologies). Data are expressed as mean of individual experiments along with the standard error of the mean. An exclusion threshold of > 3 times the standard deviation in power in some frequency bins was defined before analysis so that if a recording had exceptional (non-biological) noise, it would not disproportionally distort the results. With this criterion, we omitted one MK-801-treated GluN2D-KO animal from the two-stage statistical analysis (but retained in Fig. 3) and one GluN2C-KO animal treated with MK-801 whose inclusion would have exaggerated the genotype effect at < 20 Hz.

These results include previously published results of drug-induced power / baseline power for ketamine-treated (8/10 of the WT and 9/9 of the GluN2D-KO animals; (Sapkota et al., 2016)) and MK-801-treated (6/12 of the WT and 3/5 of the GluN2C-KO animals (Gupta et al., 2016)). These were included to provide a more complete data set for comparison with other genotypes and channel blockers and so that all of the results could be evaluated with a two-stage cluster-based permutation procedure. In this manner, each of the genotype/drug combinations could be evaluated using the same, high-stringency statistical approach. The one GluN2C-KO-MK-801-treated mouse was excluded since it met our exclusion threshold by having very large noise at low frequencies which we interpreted as non-biological. Its inclusion (as in Gupta et al., 2016), greatly distorts the average at low frequencies but did not alter the conclusions since the conclusions relate to higher frequencies.

4.5 Statistical analysis

Due to the spectral non-independence of our frequency data, traditional Bonferroni correction was inappropriate for multiple comparisons correction, as it would substantially increase the risk of Type II error. Thus, to reduce the risk of false positive results while maintaining reasonable sensitivity, a two-stage cluster-based permutation procedure was followed to control for Type I error (Ernst, 2004). Briefly, rather than assuming a standard null distribution, the cluster-based permutation approach approximates the null distribution by random permutation of the data, and thereby incorporates the autocorrelation of the data into this consideration. In the first stage, unpaired t-tests were conducted to test for differences between KO and WT mice at each data point (i.e., each frequency bin) and the output series of t-values was thresholded at $p < 0.05$ to define frequency bins containing potentially significant deviations between the groups. In stage two, the frequency bins that survived the initial threshold were clustered with spectrally neighboring bins that were also above the threshold, and a cluster value was derived by summing all of the t-values of all data points in the cluster. Ten-thousand permutations were then performed wherein the group assignments were randomized and the above clustering method was repeated, resulting in a distribution of maximum cluster-values, against which the significance level of the observed clusters (from stage one) were tested directly. A final threshold of $p < .01$ was

used to define statistical significance. Due to occasional, signal noise in the low frequencies due to cable movement, we restricted our statistical analysis to frequencies between 30 and 200 Hz.

5. Acknowledgements

This work was supported by the National Institutes of Mental Health [grants MH60252 and GM110768]. The authors thank Dr. Andres Buonanno and colleagues for having provided the GluN2C-KO mouse line and Dr. Masayoshi Mishina and colleagues for the GluN2D-KO mouse. We also thank Robin Taylor for expert graphical assistance.

7. References

Alsaad HA, DeKorver NW, Mao Z, Dravid SM, Arikkath J, Monaghan DT, 2019 In the Telencephalon, GluN2C NMDA Receptor Subunit mRNA is Predominately Expressed in Glial Cells and GluN2D mRNA in Interneurons. Neurochem Res. 44, 61–77. [PubMed: 29651654]

Angulo MC, Kozlov AS, Charpak S, Audinat E, 2004 Glutamate released from glial cells synchronizes neuronal activity in the hippocampus. J Neurosci. 24, 6920–7. [PubMed: 15295027]

Araque A, Li N, Doyle RT, Haydon PG, 2000 SNARE protein-dependent glutamate release from astrocytes. J Neurosci. 20, 666–73. [PubMed: 10632596]

Benveniste M, Mayer ML, 1991 Kinetic analysis of antagonist action at N-methyl-D-aspartic acid receptors. Two binding sites each for glutamate and glycine. Biophys J. 59, 560–73. [PubMed: 1710938]

Bezzi P, Carmignoto G, Pasti L, Vesce S, Rossi D, Rizzini BL, Pozzan T, Volterra A, 1998 Prostaglandins stimulate calcium-dependent glutamate release in astrocytes. Nature. 391, 281–5. [PubMed: 9440691]

Block AE, Dhanji H, Thompson-Tardif SF, Floresco SB, 2007 Thalamic-prefrontal cortical-ventral striatal circuitry mediates dissociable components of strategy set shifting. Cerebral cortex (New York, N.Y.: 1991). 17, 1625–1636.

Briggs CA, McKenna DG, 1996 Effect of MK-801 at the human alpha 7 nicotinic acetylcholine receptor. Neuropharmacology. 35, 407–14. [PubMed: 8793902]

Brothwell SL, Barber JL, Monaghan DT, Jane DE, Gibb AJ, Jones S, 2008 NR2B- and NR2D-containing synaptic NMDA receptors in developing rat substantia nigra pars compacta dopaminergic neurones. J Physiol. 586, 739–50. [PubMed: 18033813]

Buller AL, Larson HC, Schneider BE, Beaton JA, Morrisett RA, Monaghan DT, 1994 The molecular basis of NMDA receptor subtypes: native receptor diversity is predicted by subunit composition. J Neurosci. 14, 5471–84. [PubMed: 7916045]

Busquets-Garcia A, Gomis-Gonzalez M, Salgado-Mendialdua V, Galera-Lopez L, Puighermanal E, Martin-Garcia E, Maldonado R, Ozaita A, 2018 Hippocampal Protein Kinase C Signaling Mediates the Short-Term Memory Impairment Induced by Delta9-Tetrahydrocannabinol. Neuropsychopharmacology. 43, 1021–1031. [PubMed: 28816239]

Buzsáki G, Wang X-J, 2012 Mechanisms of gamma oscillations. Annual review of neuroscience. 35, 203–225.

Cardin JA, Carlén M, Meletis K, Knoblich U, Zhang F, Deisseroth K, Tsai L-H, Moore CI, 2009 Driving fast-spiking cells induces gamma rhythm and controls sensory responses. Nature. 459, 663–667. [PubMed: 19396156]

Carlen M, Meletis K, Siegle JH, Cardin JA, Futai K, Vierling-Claassen D, Ruhlmann C, Jones SR, Deisseroth K, Sheng M, Moore CI, Tsai LH, 2012 A critical role for NMDA receptors in parvalbumin interneurons for gamma rhythm induction and behavior. Mol Psychiatry. 17, 537–48. [PubMed: 21468034]

Cho RY, Konecky RO, Carter CS, 2006 Impairments in frontal cortical gamma synchrony and cognitive control in schizophrenia. Proc Natl Acad Sci U S A. 103, 19878–83. [PubMed: 17170134]

Clarke PB, Reuben M, 1995 Inhibition by dizocilpine (MK-801) of striatal dopamine release induced by MPTP and MPP+: possible action at the dopamine transporter. Br J Pharmacol. 114, 315–22. [PubMed: 7881731]

Clements JD, Westbrook GL, 1991 Activation kinetics reveal the number of glutamate and glycine binding sites on the N-methyl-D-aspartate receptor. Neuron. 7, 605–13. [PubMed: 1681832]

Costa BM, Feng B, Tsintsadze TS, Morley RM, Irvine MW, Tsintsadze V, Lozovaya NA, Jane DE, Monaghan DT, 2009 N-methyl-D-aspartate (NMDA) receptor NR2 subunit selectivity of a series of novel piperazine-2,3-dicarboxylate derivatives: preferential blockade of extrasynaptic NMDA receptors in the rat hippocampal CA3-CA1 synapse. J Pharmacol Exp Ther. 331, 618–26. [PubMed: 19684252]

Dalton GL, Wu DC, Wang YT, Floresco SB, Phillips AG, 2012 NMDA GluN2A and GluN2B receptors play separate roles in the induction of LTP and LTD in the amygdala and in the acquisition and extinction of conditioned fear. Neuropharmacology. 62, 797–806. [PubMed: 21925518]

Dzirasa K, Ramsey AJ, Takahashi DY, Stapleton J, Potes JM, Williams JK, Gainetdinov RR, Sameshima K, Caron MG, Nicolelis MA, 2009 Hyperdopaminergia and NMDA receptor hypofunction disrupt neural phase signaling. J Neurosci. 29, 8215–24. [PubMed: 19553461]

Ernst MD, 2004 Permutation methods: a basis for exact inference. . Statistical Science. 19, 676–685.

Fellin T, Pascual O, Gobbo S, Pozzan T, Haydon PG, Carmignoto G, 2004 Neuronal synchrony mediated by astrocytic glutamate through activation of extrasynaptic NMDA receptors. Neuron. 43, 729–43. [PubMed: 15339653]

Feng B, Tse HW, Skifter DA, Morley R, Jane DE, Monaghan DT, 2004 Structure-activity analysis of a novel NR2C/NR2D-preferring NMDA receptor antagonist: 1-(phenanthrene-2-carbonyl) piperazine-2,3-dicarboxylic acid. Br J Pharmacol. 141, 508–16. [PubMed: 14718249]

Fox CJ, Russell KI, Wang YT, Christie BR, 2006 Contribution of NR2A and NR2B NMDA subunits to bidirectional synaptic plasticity in the hippocampus in vivo. Hippocampus. 16, 907–15. [PubMed: 17024679]

Ge Y, Dong Z, Bagot RC, Howland JG, Phillips AG, Wong TP, Wang YT, 2010 Hippocampal long-term depression is required for the consolidation of spatial memory. Proc Natl Acad Sci U S A. 107, 16697–702.

Gilmour G, Pioli EY, Dix SL, Smith JW, Conway MW, Jones WT, Loomis S, Mason R, Shahabi S, Tricklebank MD, 2009 Diverse and often opposite behavioural effects of NMDA receptor antagonists in rats: implications for “NMDA antagonist modelling” of schizophrenia. Psychopharmacology (Berl). 205, 203–16. [PubMed: 19421743]

Glasgow NG, Siegler Retchless B, Johnson JW, 2015 Molecular bases of NMDA receptor subtype-dependent properties. J Physiol. 593, 83–95. [PubMed: 25556790]

Gupta SC, Ravikrishnan A, Liu J, Mao Z, Pavuluri R, Hillman BG, Gandhi PJ, Stairs DJ, Li M, Ugale RR, Monaghan DT, Dravid SM, 2016 The NMDA receptor GluN2C subunit controls cortical excitatory-inhibitory balance, neuronal oscillations and cognitive function. Sci Rep. 6, 38321. [PubMed: 27922130]

Haenschel C, Bittner RA, Waltz J, Haertling F, Wibral M, Singer W, Linden DE, Rodriguez E, 2009 Cortical oscillatory activity is critical for working memory as revealed by deficits in early-onset schizophrenia. J Neurosci. 29, 9481–9. [PubMed: 19641111]

Hagino Y, Kasai S, Han W, Yamamoto H, Nabeshima T, Mishina M, Ikeda K, 2010 Essential role of NMDA receptor channel epsilon4 subunit (GluN2D) in the effects of phencyclidine, but not methamphetamine. PLoS One. 5, e13722. [PubMed: 21060893]

Hakami T, Jones NC, Tolmacheva EA, Gaudias J, Chaumont J, Salzberg M, O’Brien TJ, Pinault D, 2009 NMDA receptor hypofunction leads to generalized and persistent aberrant gamma oscillations independent of hyperlocomotion and the state of consciousness. PLoS One. 4, e6755. [PubMed: 19707548]

Hansen KB, Ogden KK, Yuan H, Traynelis SF, 2014 Distinct functional and pharmacological properties of Triheteromeric GluN1/GluN2A/GluN2B NMDA receptors. Neuron. 81, 1084–96. [PubMed: 24607230]

Hatton CJ, Paoletti P, 2005 Modulation of triheteromeric NMDA receptors by N-terminal domain ligands. Neuron. 46, 261–74. [PubMed: 15848804]

Havolli E, Hill MD, Godley A, Goetghebeur PJ, 2017 Spatial recognition test: A novel cognition task for assessing topographical memory in mice. J Psychopharmacol. 31, 653–659. [PubMed: 28514890]

Haydon PG, 2001 GLIA: listening and talking to the synapse. Nat Rev Neurosci. 2, 185–93. [PubMed: 11256079]

Heja L, Nyitrai G, Kekesi O, Dobolyi A, Szabo P, Fiath R, Ulbert I, Pal-Szenthe B, Palkovits M, Kardos J, 2012 Astrocytes convert network excitation to tonic inhibition of neurons. BMC Biol. 10, 26. [PubMed: 22420899]

Hiyoshi T, Kambe D, Karasawa J, Chaki S, 2014 Differential effects of NMDA receptor antagonists at lower and higher doses on basal gamma band oscillation power in rat cortical electroencephalograms. Neuropharmacology. 85, 384–96. [PubMed: 24907590]

Hollmann M, Boulter J, Maron C, Beasley L, Sullivan J, Pecht G, Heinemann S, 1993 Zinc potentiates agonist-induced currents at certain splice variants of the NMDA receptor. Neuron. 10, 943–54. [PubMed: 7684237]

Homayoun H, Moghaddam B, 2007 NMDA receptor hypofunction produces opposite effects on prefrontal cortex interneurons and pyramidal neurons. J Neurosci. 27, 11496–500. [PubMed: 17959792]

Hong LE, Summerfelt A, Buchanan RW, O'Donnell P, Thaker GK, Weiler MA, Lahti AC, 2010 Gamma and delta neural oscillations and association with clinical symptoms under subanesthetic ketamine. Neuropsychopharmacology. 35, 632–40. [PubMed: 19890262]

Hu M, Sun YJ, Zhou QG, Auberson YP, Chen L, Hu Y, Luo CX, Wu JY, Zhu DY, Li LX, 2009 Reduced spatial learning in mice treated with NVP-AAM077 through down-regulating neurogenesis. Eur J Pharmacol. 622, 37–44. [PubMed: 19765576]

Hunt MJ, Raynaud B, Garcia R, 2006 Ketamine dose-dependently induces high-frequency oscillations in the nucleus accumbens in freely moving rats. Biological psychiatry. 60, 1206–1214. [PubMed: 16650831]

Hunt MJ, Kasicki S, 2013 A systematic review of the effects of NMDA receptor antagonists on oscillatory activity recorded in vivo. J Psychopharmacol. 27, 972–86. [PubMed: 23863924]

Ikeda K, Nagasawa M, Mori H, Araki K, Sakimura K, Watanabe M, Inoue Y, Mishina M, 1992 Cloning and expression of the epsilon 4 subunit of the NMDA receptor channel. FEBS Lett. 313, 34–8. [PubMed: 1385220]

Jeffrey M, Lang M, Gane J, Wu C, Burnham WM, Zhang L, 2013 A reliable method for intracranial electrode implantation and chronic electrical stimulation in the mouse brain. BMC Neurosci. 14, 82. [PubMed: 23914984]

Kakefuda K, Ishisaka M, Tsuruma K, Shimazawa M, Hara H, 2016 Memantine, an NMDA receptor antagonist, improves working memory deficits in DGKbeta knockout mice. Neurosci Lett. 630, 228–232. [PubMed: 27495014]

Kantrowitz JT, Javitt DC, 2010 N-methyl-d-aspartate (NMDA) receptor dysfunction or dysregulation: the final common pathway on the road to schizophrenia? Brain Res Bull. 83, 108–21. [PubMed: 20417696]

Kikuchi M, Hashimoto T, Nagasawa T, Hirosawa T, Minabe Y, Yoshimura M, Strik W, Dierks T, Koenig T, 2011 Frontal areas contribute to reduced global coordination of resting-state gamma activities in drug-naive patients with schizophrenia. Schizophr Res. 130, 187–94. [PubMed: 21696922]

Kocsis B, 2012a State-dependent increase of cortical gamma activity during REM sleep after selective blockade of NR2B subunit containing NMDA receptors. Sleep. 35, 1011–6. [PubMed: 22754048]

Kocsis B, 2012b Differential role of NR2A and NR2B subunits in N-methyl-D-aspartate receptor antagonist-induced aberrant cortical gamma oscillations. Biol Psychiatry. 71, 987–95. [PubMed: 22055014]

Korotkova T, Fuchs EC, Ponomarenko A, von Engelhardt J, Monyer H, 2010 NMDA receptor ablation on parvalbumin-positive interneurons impairs hippocampal synchrony, spatial representations, and working memory. Neuron. 68, 557–69. [PubMed: 21040854]

Kotermanski SE, Johnson JW, 2009 Mg2+ imparts NMDA receptor subtype selectivity to the Alzheimer's drug memantine. J Neurosci. 29, 2774–9. [PubMed: 19261873]

Krupp JJ, Vissel B, Heinemann SF, Westbrook GL, 1998 N-terminal domains in the NR2 subunit control desensitization of NMDA receptors. Neuron. 20, 317–27. [PubMed: 9491992]

Lee HS, Ghetti A, Pinto-Duarte A, Wang X, Dziewczapolski G, Galimi F, Huitron-Resendiz S, Pina-Crespo JC, Roberts AJ, Verma IM, Sejnowski TJ, Heinemann SF, 2014 Astrocytes contribute to gamma oscillations and recognition memory. Proc Natl Acad Sci U S A. 111, E3343–52. [PubMed: 25071179]

Lesuis SL, Lucassen PJ, Krugers HJ, 2019 Early life stress impairs fear memory and synaptic plasticity; a potential role for GluN2B. Neuropharmacology. 149, 195–203. [PubMed: 30641077]

Li Q, Clark S, Lewis DV, Wilson WA, 2002 NMDA receptor antagonists disinhibit rat posterior cingulate and retrosplenial cortices: a potential mechanism of neurotoxicity. J Neurosci. 22, 3070–80. [PubMed: 11943810]

Lisman JE, Coyle JT, Green RW, Javitt DC, Benes FM, Heckers S, Grace AA, 2008 Circuit-based framework for understanding neurotransmitter and risk gene interactions in schizophrenia. Trends Neurosci. 31, 234–42. [PubMed: 18395805]

Lohani S, Martig AK, Deisseroth K, Witten IB, Moghaddam B, 2019 Dopamine Modulation of Prefrontal Cortex Activity Is Manifold and Operates at Multiple Temporal and Spatial Scales. Cell Rep. 27, 99–114 e6. [PubMed: 30943418]

Lozovaya NA, Grebenyuk SE, Tsintsadze T, Feng B, Monaghan DT, Krishtal OA, 2004 Extrasynaptic NR2B and NR2D subunits of NMDA receptors shape 'superslow' afterburst EPSC in rat hippocampus. J Physiol. 558, 451–63. [PubMed: 15146049]

Mancarci BO, Toker L, Tripathy SJ, Li B, Rocco B, Sibille E, Pavlidis P, 2017 Cross-laboratory analysis of brain cell type transcriptomes with applications to interpretation of bulk tissue data. eNeuro. ENEURO. 0212–17. 2017.

Masu M, Nakajima Y, Moriyoshi K, Ishii T, Akazawa C, Nakanashi S, 1993 Molecular characterization of NMDA and metabotropic glutamate receptors. Ann N Y Acad Sci. 707, 153–64. [PubMed: 9137550]

Mikics E, Toth M, Biro L, Bruzsik B, Nagy B, Haller J, 2017 The role of GluN2B-containing NMDA receptors in short- and long-term fear recall. Physiol Behav. 177, 44–48. [PubMed: 28400283]

Mishina M, Mori H, Araki K, Kushiya E, Meguro H, Kutsuwada T, Kashiwabuchi N, Ikeda K, Nagasawa M, Yamazaki M, et al., 1993 Molecular and functional diversity of the NMDA receptor channel. Ann N Y Acad Sci. 707, 136–52. [PubMed: 9137549]

Monyer H, Burnashev N, Laurie DJ, Sakmann B, Seeburg PH, 1994 Developmental and regional expression in the rat brain and functional properties of four NMDA receptors. Neuron. 12, 529–40. [PubMed: 7512349]

Palygin O, Lalo U, Verkhratsky A, Pankratov Y, 2010 Ionotropic NMDA and P2X1/5 receptors mediate synaptically induced Ca2+ signalling in cortical astrocytes. Cell Calcium. 48, 225–31. [PubMed: 20926134]

Palygin O, Lalo U, Pankratov Y, 2011 Distinct pharmacological and functional properties of NMDA receptors in mouse cortical astrocytes. Br J Pharmacol. 163, 1755–66. [PubMed: 21449975]

Paoletti P, Bellone C, Zhou Q, 2013 NMDA receptor subunit diversity: impact on receptor properties, synaptic plasticity and disease. Nat Rev Neurosci. 14, 383–400. [PubMed: 23686171]

Pasti L, Zonta M, Pozzan T, Vicini S, Carmignoto G, 2001 Cytosolic calcium oscillations in astrocytes may regulate exocytotic release of glutamate. J Neurosci. 21, 477–84. [PubMed: 11160427]

Perszyk RE, DiRaddo JO, Strong KL, Low CM, Ogden KK, Khatri A, Vargish GA, Pelkey KA, Tricoire L, Liotta DC, Smith Y, McBain CJ, Traynelis SF, 2016 GluN2D-Containing N-methyl-d-Aspartate Receptors Mediate Synaptic Transmission in Hippocampal Interneurons and Regulate Interneuron Activity. Mol Pharmacol. 90, 689–702. [PubMed: 27625038]

Phillips KG, Cotel MC, McCarthy AP, Edgar DM, Tricklebank M, O'Neill MJ, Jones MW, Wafford KA, 2012 Differential effects of NMDA antagonists on high frequency and gamma EEG oscillations in a neurodevelopmental model of schizophrenia. Neuropharmacology. 62, 1359–70. [PubMed: 21521646]

Pinault D, 2008 N-methyl d-aspartate receptor antagonists ketamine and MK-801 induce wake-related aberrant gamma oscillations in the rat neocortex. Biol Psychiatry. 63, 730–5. [PubMed: 18022604]

Pittman-Polletta B, Hu K, Kocsis B, 2018 Subunit-specific NMDAR antagonism dissociates schizophrenia subtype-relevant oscillopathies associated with frontal hypofunction and hippocampal hyperfunction. Sci Rep. 8, 11588.

Povysheva NV, Johnson JW, 2012 Tonic NMDA receptor-mediated current in prefrontal cortical pyramidal cells and fast-spiking interneurons. J Neurophysiol. 107, 2232–43. [PubMed: 22236713]

Ravikrishnan A, Gandhi PJ, Shelkar GP, Liu J, Pavuluri R, Dravid SM, 2018 Region-specific Expression of NMDA Receptor GluN2C Subunit in Parvalbumin-Positive Neurons and Astrocytes: Analysis of GluN2C Expression using a Novel Reporter Model. Neuroscience. 380, 49–62. [PubMed: 29559384]

Riebe I, Seth H, Culley G, Dosa Z, Radi S, Strand K, Frojd V, Hanse E, 2016 Tonically active NMDA receptors--a signalling mechanism critical for interneuronal excitability in the CA1 stratum radiatum. Eur J Neurosci. 43, 169–78. [PubMed: 26547631]

Sapkota K, Mao Z, Synowicki P, Lieber D, Liu M, Ikezu T, Gautam V, Monaghan DT, 2016 GluN2D N-Methyl-d-Aspartate Receptor Subunit Contribution to the Stimulation of Brain Activity and Gamma Oscillations by Ketamine: Implications for Schizophrenia. J Pharmacol Exp Ther. 356, 702–11. [PubMed: 26675679]

Sato Y, Kobayashi E, Hakamata Y, Kobahashi M, Wainai T, Murayama T, Mishina M, Seo N, 2004 Chronopharmacological studies of ketamine in normal and NMDA epsilon1 receptor knockout mice. Br J Anaesth. 92, 859–64. [PubMed: 15064251]

Shelkar GP, Pavuluri R, Gandhi PJ, Ravikrishnan A, Gawande DY, Liu J, Stairs DJ, Ugale RR, Dravid SM, 2019 Differential effect of NMDA receptor GluN2C and GluN2D subunit ablation on behavior and channel blocker-induced schizophrenia phenotypes. Sci Rep. 9, 7572. [PubMed: 31110197]

Sleigh J, Harvey M, Voss L, Denny B, 2014 Ketamine-More mechanisms of action than just NMDA blockade. Trends in anaesthesia and critical care. 4, 76–81.

Spencer KM, Nestor PG, Niznikiewicz MA, Salisbury DF, Shenton ME, McCarley RW, 2003 Abnormal neural synchrony in schizophrenia. J Neurosci. 23, 7407–11. [PubMed: 12917376]

Spencer KM, Salisbury DF, Shenton ME, McCarley RW, 2008 Gamma-band auditory steady-state responses are impaired in first episode psychosis. Biol Psychiatry. 64, 369–75. [PubMed: 18400208]

Spencer KM, Niznikiewicz MA, Nestor PG, Shenton ME, McCarley RW, 2009 Left auditory cortex gamma synchronization and auditory hallucination symptoms in schizophrenia. BMC Neurosci. 10, 85. [PubMed: 19619324]

Spencer KM, 2011 Baseline gamma power during auditory steady-state stimulation in schizophrenia. Front Hum Neurosci. 5, 190. [PubMed: 22319485]

Standaert DG, Friberg IK, Landwehrmeyer GB, Young AB, Penney JB Jr., 1999 Expression of NMDA glutamate receptor subunit mRNAs in neurochemically identified projection and interneurons in the striatum of the rat. Brain Res Mol Brain Res. 64, 11–23. [PubMed: 9889300]

Sugihara H, Moriyoshi K, Ishii T, Masu M, Nakanishi S, 1992 Structures and properties of seven isoforms of the NMDA receptor generated by alternative splicing. Biochem Biophys Res Commun. 185, 826–32. [PubMed: 1352681]

Tan Z, Liu Y, Xi W, Lou HF, Zhu L, Guo Z, Mei L, Duan S, 2017 Glia-derived ATP inversely regulates excitability of pyramidal and CCK-positive neurons. Nat Commun. 8, 13772. [PubMed: 28128211]

Traynelis SF, Wollmuth LP, McBain CJ, Menniti FS, Vance KM, Ogden KK, Hansen KB, Yuan H, Myers SJ, Dingledine R, 2010 Glutamate receptor ion channels: structure, regulation, and function. Pharmacol Rev. 62, 405–96. [PubMed: 20716669]

Uhlhaas PJ, Haenschel C, Nikolic D, Singer W, 2008 The role of oscillations and synchrony in cortical networks and their putative relevance for the pathophysiology of schizophrenia. Schizophr Bull. 34, 927–43. [PubMed: 18562344]

Uhlhaas PJ, Singer W, 2012 Neuronal dynamics and neuropsychiatric disorders: toward a translational paradigm for dysfunctional large-scale networks. Neuron. 75, 963–80. [PubMed: 22998866]

Uhlhaas PJ, Singer W, 2015 Oscillations and neuronal dynamics in schizophrenia: the search for basic symptoms and translational opportunities. Biol Psychiatry. 77, 1001–9. [PubMed: 25676489]

Verkhratsky A, Orkand RK, Kettenmann H, 1998 Glial calcium: homeostasis and signaling function. Physiol Rev. 78, 99–141. [PubMed: 9457170]

Vicini S, Wang JF, Li JH, Zhu WJ, Wang YH, Luo JH, Wolfe BB, Grayson DR, 1998 Functional and pharmacological differences between recombinant N-methyl- D-aspartate receptors. J Neurophysiol. 79, 555–66. [PubMed: 9463421]

von Engelhardt J, Bocklisch C, Tonges L, Herb A, Mishina M, Monyer H, 2015 GluN2D-containing NMDA receptors-mediate synaptic currents in hippocampal interneurons and pyramidal cells in juvenile mice. Front Cell Neurosci. 9, 95. [PubMed: 25859181]

Watanabe M, Inoue Y, Sakimura K, Mishina M, 1992 Developmental changes in distribution of NMDA receptor channel subunit mRNAs. Neuroreport. 3, 1138–40. [PubMed: 1493227]

Watanabe M, Inoue Y, Sakimura K, Mishina M, 1993a Distinct distributions of five N-methyl-D-aspartate receptor channel subunit mRNAs in the forebrain. J Comp Neurol. 338, 377–90. [PubMed: 8113446]

Watanabe M, Inoue Y, Sakimura K, Mishina M, 1993b Distinct Spatio-temporal Distributions of the NMDA Receptor Channel Subunit mRNAs in the Brain. Annals of the New York Academy of Sciences. 707, 463–466. [PubMed: 9137596]

Wyllie DJ, Livesey MR, Hardingham GE, 2013 Influence of GluN2 subunit identity on NMDA receptor function. Neuropharmacology. 74, 4–17. [PubMed: 23376022]

Yamamoto T, Nakayama T, Yamaguchi J, Matsuzawa M, Mishina M, Ikeda K, Yamamoto H, 2016 Role of the NMDA receptor GluN2D subunit in the expression of ketamine-induced behavioral sensitization and region-specific activation of neuronal nitric oxide synthase. Neuroscience Letters. 610, 48–53. [PubMed: 26520463]

Yamasaki M, Okada R, Takasaki C, Toki S, Fukaya M, Natsume R, Sakimura K, Mishina M, Shirakawa T, Watanabe M, 2014 Opposing role of NMDA receptor GluN2B and GluN2D in somatosensory development and maturation. J Neurosci. 34, 11534–48. [PubMed: 25164652]

Yu X, Jia L, Yin K, Lv J, Yu W, Du H, 2018 Src is Implicated in Hepatic Ischemia Reperfusion-Induced Hippocampus Injury and Long-Term Cognitive Impairment in Young Mice via NMDA Receptor Subunit 2A Activation. Neuroscience. 391, 1–12. [PubMed: 30213765]

Zhang L, Xu T, Wang S, Yu L, Liu D, Zhan R, Yu SY, 2013 NMDA GluN2B receptors involved in the antidepressant effects of curcumin in the forced swim test. Prog Neuropsychopharmacol Biol Psychiatry. 40, 12–7. [PubMed: 22960607]

Zhang Y, Chen K, Sloan SA, Bennett ML, Scholze AR, O'Keeffe S, Phatnani HP, Guarnieri P, Caneda C, Ruderisch N, Deng S, Liddelow SA, Zhang C, Daneman R, Maniatis T, Barres BA, Wu JQ, 2014 An RNA-sequencing transcriptome and splicing database of glia, neurons, and vascular cells of the cerebral cortex. J Neurosci. 34, 11929–47. [PubMed: 25186741]

Zhu G, Li J, He L, Wang X, Hong X, 2015 MPTP-induced changes in hippocampal synaptic plasticity and memory are prevented by memantine through the BDNF-TrkB pathway. Br J Pharmacol. 172, 2354–68. [PubMed: 25560396]

Highlights:

- NMDA receptor channel blockers induced stronger neuronal oscillations in GluN2C knockout mice.
- NMDA receptor channel blockers induced weaker neuronal oscillations in GluN2D knockout mice.
- NVP-AAM077 and Ro 25–6981induced oscillations appear to be unchanged in GluN2C and GluN2D knockouts.
- GluN2C/D-containing NMDARs may be modulating oscillations through bidirectional feedback.

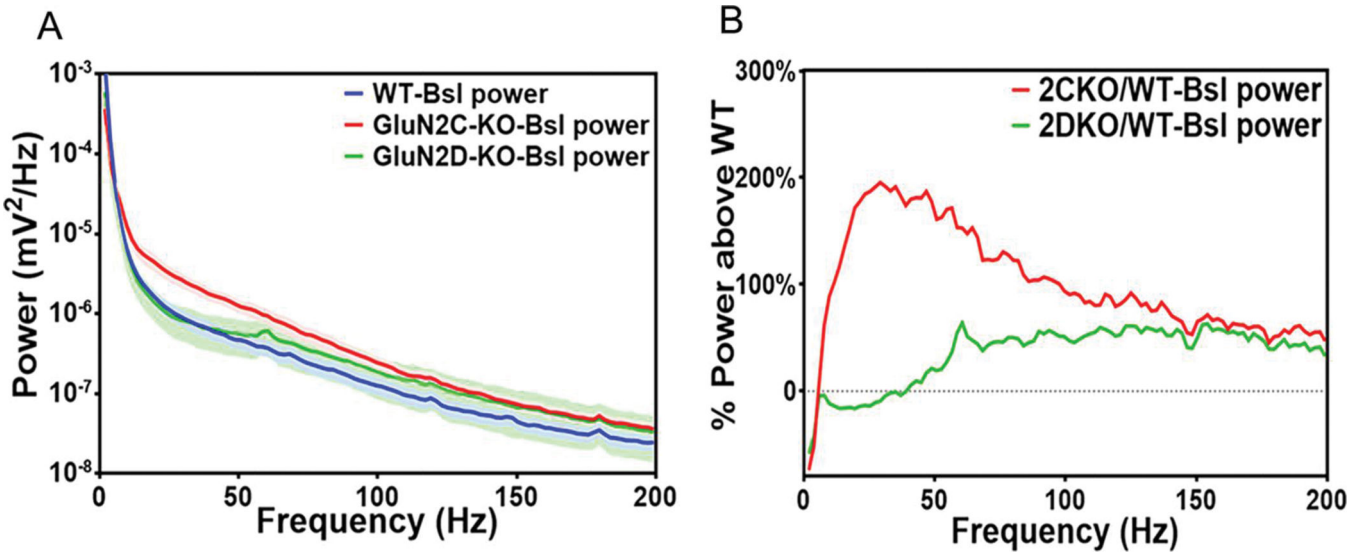

Figure 1.

Baseline oscillations in GluN2C-KO, and GluN2D-KO mice. (A): ECoG analysis of baseline power spectrum of WT, GluN2C-KO, GluN2D-KO animals before drug administration. SEMs are shown by light shading. (B): % Power of oscillations in GluN2C-KO and GluN2D-KO mice compared to WT mice.

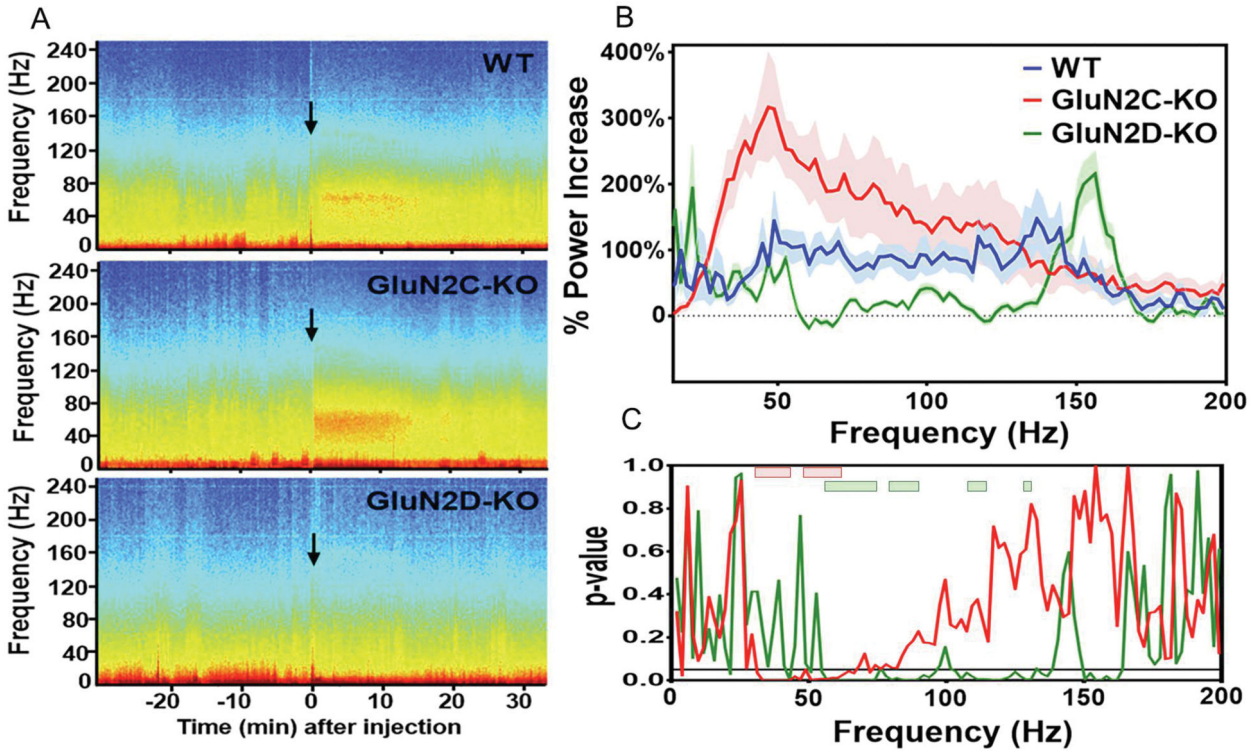

Figure 2.

Ketamine-induced oscillations in WT, GluN2C-KO and GluN2D-KO mice. (A): Representative time-frequency spectrograms of ketamine effects in WT, GluN2C-KO, and GluN2D-KO mice. Ketamine was injected at time = 0 (arrow). (B): The average % increase in oscillatory power is shown for different frequencies in response to ketamine injection for WT (blue line, n = 10), GluN2C-KO (red line, n = 6), and GluN2D-KO (green line, n = 9) mice. The dotted line represents 0% increase, no drug-induced change in power. SEMs are shown by light shading. (C): The statistical significance of the difference between WT and KO animals in oscillatory power at different frequencies is shown by a graph of the p values, the solid line represents p = 0.05. The shaded boxes indicate frequency clusters that were statistically significant ($p<0.001$) after cluster/permutation analysis for differences between WT and GluN2C-KO (pink) and between WT and GluN2D-KO (green).

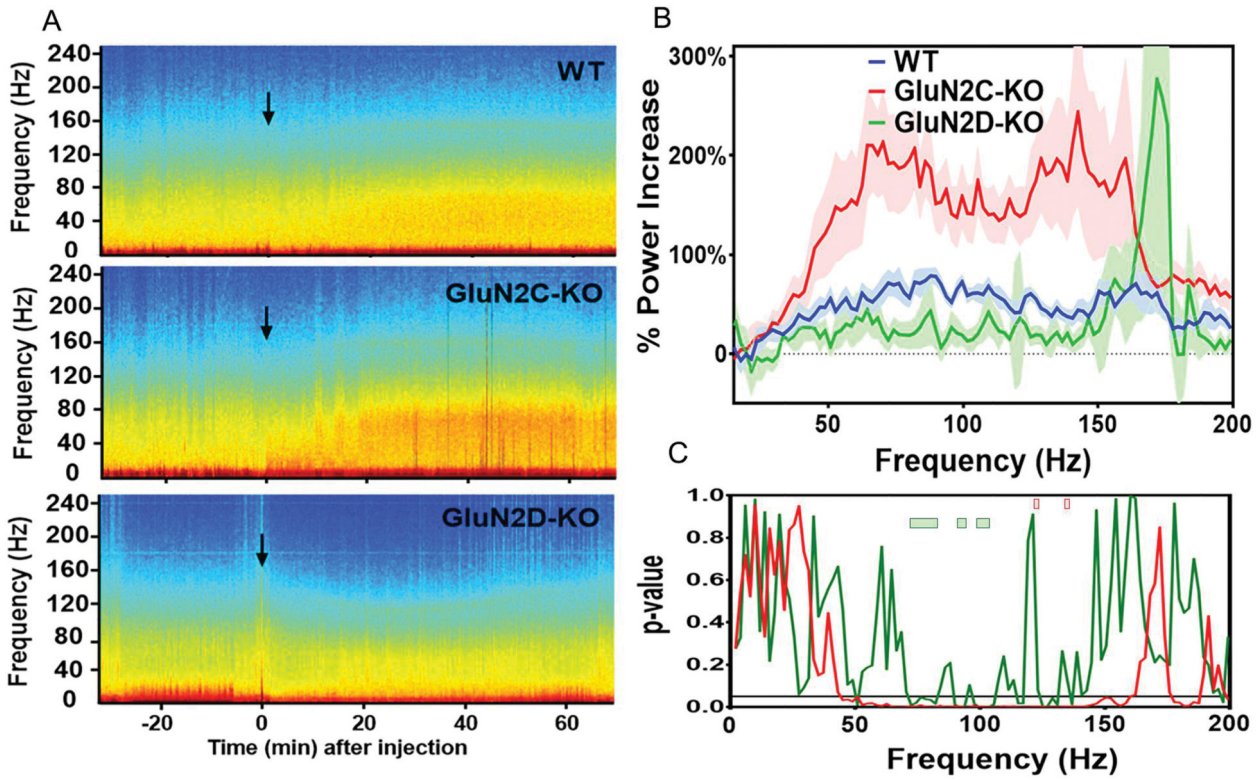

Figure 3.

MK-801-induced oscillations in WT, GluN2C-KO and GluN2D-KO mice (A): Representative time-frequency spectrograms of MK-801 effects; MK-801 was injected at time = 0 (arrow). (B): The average % increase in oscillatory power is shown for different frequencies in response to MK-801 injection for WT (blue line, n = 12), GluN2C-KO (red line, n = 5), and GluN2D-KO (green line, n = 9) mice. The dotted line represents 0% increase. SEMs are shown by light shading. (C): The statistical significance of the difference between WT and KO animals in oscillatory power at different frequencies is shown by a graph of the p values, the solid line represents p = 0.05. The shaded boxes indicate frequency clusters that were statistically significant ($p < 0.001$, except the WT-GluN2C cluster at 131–133 Hz, $p = 0.0013$) after cluster/permutation analysis for differences between WT and GluN2C-KO (pink) and between WT and GluN2D-KO (green).

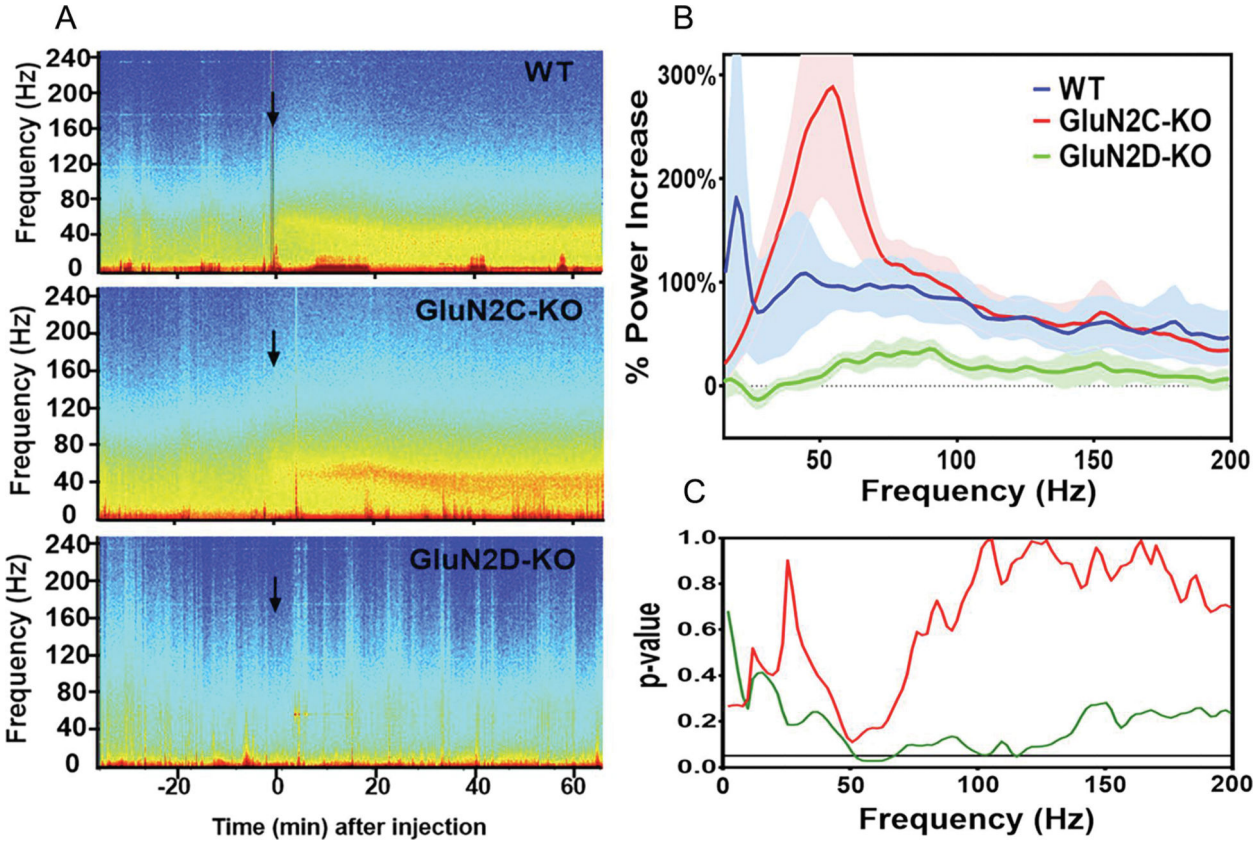

Figure 4.

PCP-induced oscillations in WT, GluN2C-KO and GluN2D-KO mice. (A): Representative time-frequency spectrograms of PCP effects; PCP injected at time = 0 (arrow). (B): The average % increase in oscillatory power is shown for different frequencies in response to PCP injection for WT (blue line, n = 5), GluN2C-KO (red line, n = 5), and GluN2D-KO (green line, n = 4) mice. SEMs are shown by light shading. (C): The statistical significance of the difference between WT and KO animals in oscillatory power at different frequencies is shown by a graph of the p values, the solid line represents p = 0.05.

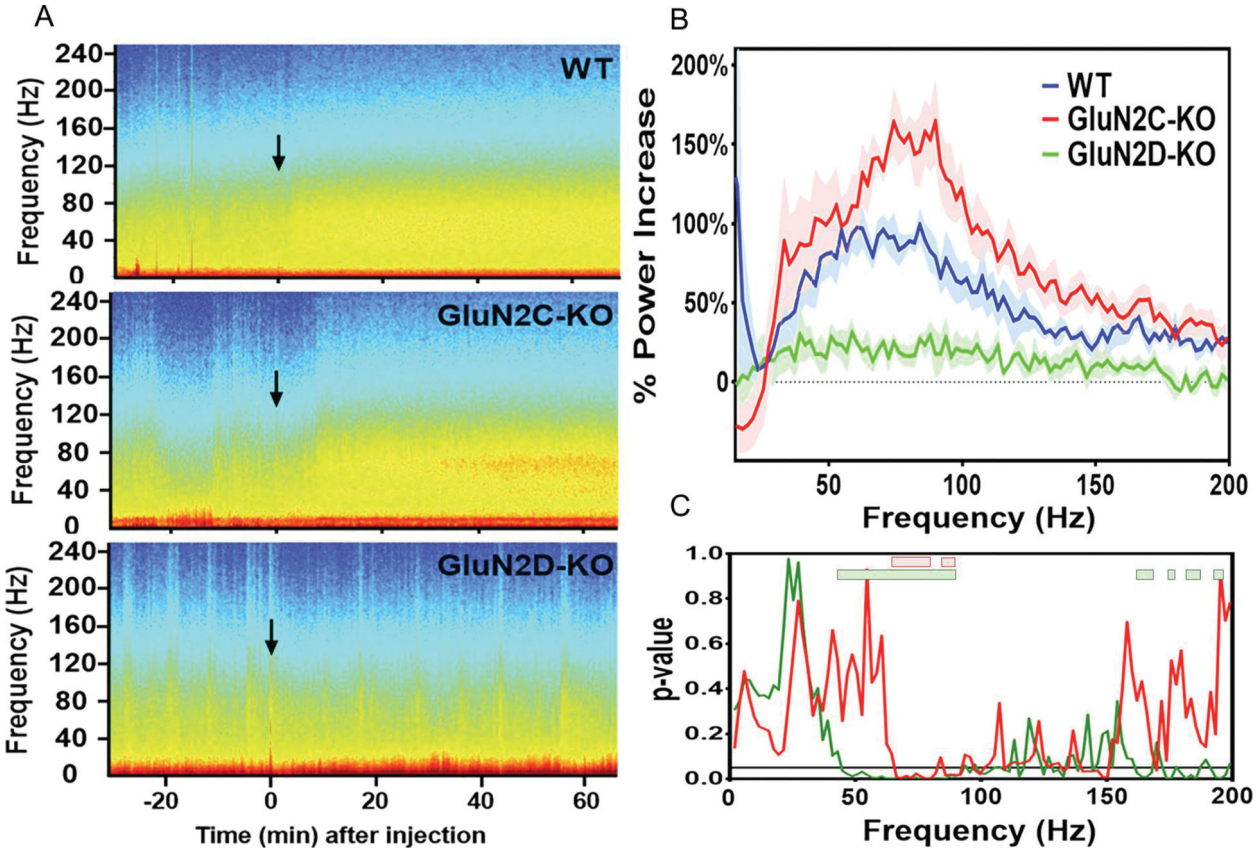

Figure 5.

Memantine-induced oscillations in GluN2C-KO and GluN2D-KO mice. (A): Representative time-frequency spectrograms of WT, GluN2C-KO, and GluN2D-KO mice. Memantine was injected at time = 0 (arrow). (B): The average % increase in oscillatory power is shown for different frequencies in response to memantine injection for WT (blue line, n = 5), GluN2C-KO (red line, n = 5), and GluN2D-KO (green line, n = 4) mice. The dotted line represents 0% increase, no drug-induced change in power. SEMs are shown by light shading. (C): The statistical significance of the difference between WT and KO animals in oscillatory power at different frequencies is shown by a graph of the p values, the solid line represents $p = 0.05$. The shaded boxes indicate frequency clusters that were statistically significant at $p < 0.001$ (except $p = 0.0025$ for WT/GluN2D at 174–176 Hz) after cluster/permutation analysis for differences between WT and GluN2C-KO (pink) and between WT and GluN2D-KO (green).

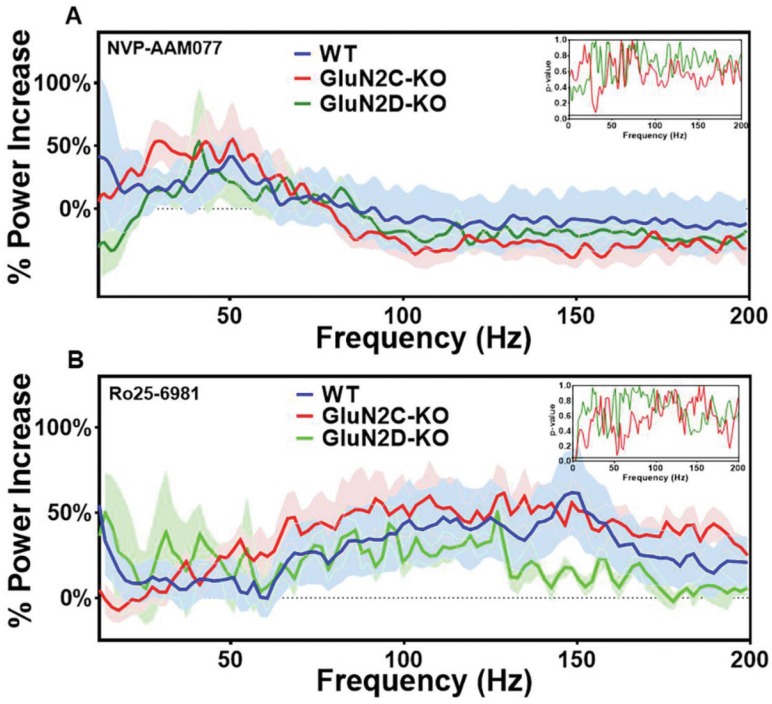

Figure 6.

(A): The average increase in NVP-AAM077-induced oscillatory power relative to the proceeding baseline condition as a function of frequency in WT (blue, n = 6), GluN2C-KO (red, n = 4) and GluN2D-KO mice (green, n = 4). (B): Ro25–6981-induced increases in oscillations in WT (blue, n = 12), GluN2C-KO (red, n = 7), and GluN2D-KO mice (green, n = 3). The dotted line represents 0% increase, no drug-induced change in power. SEMs are shown by light shading. Insert figure shows the statistical significance of the difference between WT and KO animals in oscillatory power at different frequencies as shown by a graph of the p values, the solid line represents p = 0.05.